Changes in the protein spectrum of mitochondria isolated from hydroxycamptothecin-treated hepatoma cells

Yu-Rong Fu[a,*], Zheng-Jun Yi[b,*], Yu-Rong Yan[a] and Zong-Yin Qiu[a]

As one of the most potent topoisomerase inhibitors, hydroxycamptothecin is more active and less toxic than conventional camptothecin. Recently, we found that hydroxycamptothecin can induce cell apoptosis via the mitochondrial pathway. This study was designed to investigate the mitochondrial protein profile in HCPT-treated cells using high-accuracy and high-sensitivity protein-identification technology. Of the 39 mitochondrial protein spots investigated, 25 displayed elevated and 14 suppressed abundance in hydroxycamptothecin-treated cells. The 25 spots were identified by mass spectrometry and they included proteins involved in many essential cellular functions. The potential role of these proteins in hydroxycamptothecin-mediated apoptosis is also discussed. This study has produced a short list of mitochondrial proteins that might hold the key to the mechanism by which hydroxycamptothecin induces mitochondrial dysfunction and cell apoptosis. It has laid the foundation for further elucidating the role of hydroxycamptothecin during apoptosis. Successful applications of multiple techniques including two-dimensional gel electrophoresis, matrix-assisted laser desorption ionization time-of-flight mass spectrometry and Western blot analysis have demonstrated that proteomic analyses provide appropriate approaches for understanding of the roles of anticancer drugs.
Anti-Cancer Drugs **18:1045–1052** © **2007 Lippincott Williams & Wilkins.**

Anti-Cancer Drugs 2007, **18:**1045–1052

Keywords: apoptosis, hydroxycamptothecin, mitochondria, proteome

[a]Department of Laboratory Medicine, Key Laboratory of Laboratory Medical Diagnostics of Ministry of Education, Chongqing University of Medical Science, Chongqing and [b]Department of Laboratory Medicine, Weifang University of Medical Science, Weifang, PRC

Correspondence to Professor Zong-Yin Qiu, Department of Laboratory Medicine, Chongqing University of Medical Science, Chongqing, PRC
Tel: +86 023 68485727; e-mail: mingdongfang@sina.com

Sponsorship: This work was supported by the grant from the National Natural Science Foundation of China (no. 30470786).

*Yu-Rong Fu and Zheng-Jun Yi have contributed equally to this work.

Received 7 December 2006 **Accepted** 6 May 2007

Introduction

Hydroxycamptothecin (HCPT), a natural analog of camptothecin, was extracted from *Camptotheca acuminata* Decne, which is a native plant of China [1]. An increasing amount of evidence supports the fact that HCPT is more active and less toxic than camptothecin [2]. Recently, HCPT has been subjected to clinical trials in the treatment of human gastric tumors [3].

Previous studies considered the inhibition of topoisomerase I activity as the only mechanism by which HCPT induced cell apoptosis; however, a considerable amount of evidence suggests that additional mechanisms might be involved in HCPT-mediated cell death.

Mitochondria play an important role in the initiation of apoptosis [4], including the loss of mitochondrial transmembrane potential and the release of apoptosis-related proteins (such as cytochrome *c*) in the early stages of apoptosis [5]. Recently, we found that HCPT induced apoptosis in hepatoma SMMC-7721 cells via the mitochondrial pathway [6].

Recent developments in proteomic techniques have opened the path towards a deeper exploration and better understanding of mitochondrial variations in structure and function. Until now, the most widely used proteomic approaches have included two-dimensional (2D) electrophoresis and mass spectrometry analysis [7]. Subcellular proteomics, as an important step towards functional proteomics, has become a focus of proteomic research. In this report, we have used proteomic approaches for the first time to characterize changes in the mitochondrial proteome, in the presence of HCPT.

Materials and methods

Materials

Iodoacetamide, ammonium bicarbonate (AB), trifluoroacetic acid and α-cyano-4-hydroxycinnamic acid were purchased from Sigma (St Louis, Missouri, USA). Acetonitrile was purchased from Fisher (Fair Lawn, New Jersey, USA). Trypsin (modified, sequencing grade, lyophilized) was purchased from Promega (Hercules, California, USA). Immobilized pH gradient (IPG) strips, acrylamide/bis (40%, 29:1) and other commonly used

0959-4973

reagents were purchased from Bio-Rad (Hercules, California, USA), unless otherwise indicated.

Cell treatment and detection of mitochondrial alterations

Hepatoma SMMC-7721 cells (#TCHu 52), obtained from the Shanghai Cell Bank of the Chinese Academy of Sciences, were cultured in RPMI-1640 medium (Gibco BRL, Grand Island, New York, USA) supplemented with 10% heat-inactivated (56°C, 30 min) fetal calf serum (Hyclone, Logan, Utah, USA).

Measurement of mitochondrial membrane potential (MMP) was performed as described previously [8] with a MitoCapture mitochondrial apoptosis detection kit (Biovision, Mountain View, California, USA). Briefly, exponentially growing cells in the presence or the absence of 0.22 μmol/l of HCPT were incubated with a MitoCapture solution at 37°C for 30 min, mounted onto slides and then imaged under a fluorescence microscope.

Confocal laser scanning microscopy was used to observe the release of cytochrome *c* from mitochondria. Cells were cultured on poly-L-lysine coverslips (BD BioCoat, San Diego, California, USA) and treated with HCPT for 6 h. Following fixation with 4% paraformaldehyde in phosphate-buffered saline, the cells were probed sequentially with primary and fluorescent-labeled secondary antibodies. Coverslips were mounted onto glass slides and imaged using a Leica laser-scanning confocal microscope (TCS SP2; Leica TCS SP2; Leica Microsystems Heidelberg, Germany). HSP60 was used as the mitochondrial marker.

Purification of mitochondria from SMMC-7721 cells

Mitochondria purification was performed according to the instructions of the mitochondria isolation kit (Pierce, Rockford, Illinois, USA). Isolated mitochondria were identified by Janus green B staining. Briefly, separated mitochondria were mounted onto glass slides, incubated with 0.1% Janus green B solution for 10 min and then visualized under a light microscope.

Contaminations from cytosol, nuclei and lysosomes were monitored by Western blot. Actin, histone and cathepsin-D were used as cytosolic, nuclear and lysosomal markers, respectively.

Two-dimensional gel electrophoresis of mitochondrial proteins

To more fully represent the entire proteome, sequential extraction (Bio-Rad, Richmond, California, USA) was applied to separate the mitochondrial proteins into two different fractions, on the basis of their differing solubilities. Briefly, reagent 1 [8 mol/l urea; 4% 3-cholamidopropyl)dimethylammonio]-l-propanesulfonate

Fig. 1

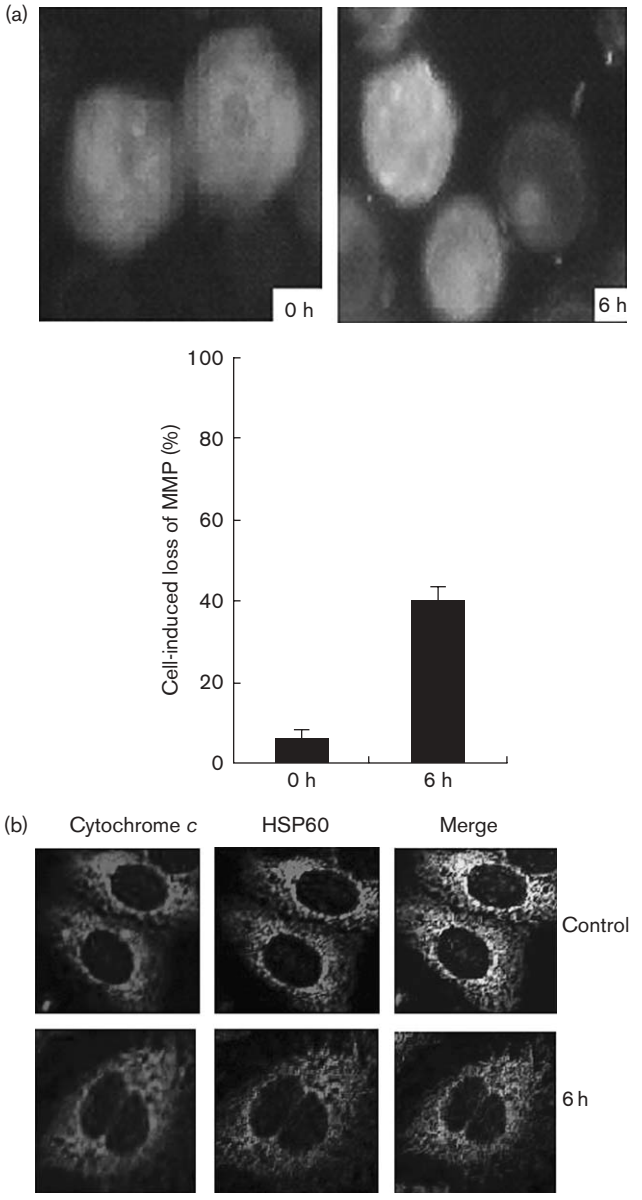

Evaluation of mitochondrial changes in HCPT-treated cells. (a) SMMC-7721cells were incubated for 6 h in the presence or the absence of 0.22 μmol/l HCPT and MMP was estimated by fluorescence microscope using the fluorescent probe MitoCapture. Control cells showed orange fluorescence, whereas the treated cells' loss of MMP showed green fluorescence. MMPs in HCPT-treated cells were decreased compared with those in control cells ($P<0.05$). Four independent assays were performed and data shown are the mean ± SD of the means obtained from triplicates of each experiment. Two-tailed analysis of variance test was used for analysis. Data shown are representative of four independent experiments (magnification: × 400). (b), Confocal microscope analysis of cytochrome *c* release from mitochondria to cytosol. The immunolocation of cytochrome *c* was in the mitochondria. After treatment with HCPT for 6 h, cytochrome *c* was translocated into the cytosol. Data shown are representative of four independent experiments (magnification: micron bar was 61.52 μm). HCPT, hydroxycamptothecin; MMP, mitochondrial membrane potential.

(CHAPS); 40 mmol/l Tris; 0.2% Bio-Lyte 3/10 ampholyte; and 2 mmol/l tributyl phosphate] was used to extract proteins of intermediate solubility and the extraction was named the 1 fraction, whereas reagent 2 (5 mol/l urea; 2 mol/l thiourea; 2% CHAPS; 2% SB 3-10; 40 mmol/l Tris; 0.2% Bio-Lyte 3/10 ampholyte; and 2 mmol/l TATA-binding protein) was used to extract proteins that were otherwise insoluble in reagent 1, and the extraction was named fraction 2. The resulting samples were diluted into a Bio-Rad 2D sample buffer with the final volume of 380 µl. IPG strips of 17 cm with pH ranges of 3–10 (Bio-Rad) were used and the strips were rehydrated at room temperature overnight. The rehydrated IPG strips were focused onto a Bio-Rad Protean IEF System, according to the manufacturer's instructions, and then reduced and alkylated before running in the second dimension on 12% SDS–PAGE gels. Gels were later fixed in 40% MeOH/10% HOAc for 1 h and stained using a Bio-Rad Silver Stain; and were then scanned as TIFF format images by a Kodak EDAS 290 scanner (Kodak, EDAS 290; Eastman Kodak, Rochester, New York, USA). Two-dimensional gel images were analyzed by PDQuest software (Bio-Rad) to compare the 2D gels of the control and the HCPT-treated groups. A statistical analysis was performed by an unpaired Student's *t*-test. The protein spots with *P* values less than 0.05 were considered as those displaying significant changes between control and HCPT-treated cells.

In-gel tryptic digestion

Spots of interest were excised and destained thoroughly, followed by reduction with 20 mmol/l of DTT in 25 mmol/l of AB (pH 8.0). The gel pieces were alkylated with 40 mmol/l iodoacetamide in 25 mmol/l AB (pH 8.0). After washing in 25 mmol/l AB and 25 mmol/l AB/50% acetonitrile, the gel pieces were digested with 40 mmol/l AB, 0.02 µg/µl trypsin (pH 8.0) for 16 h at 37°C.

Protein identification and data analysis

Peptide samples resulting from the in-gel digest were analyzed on a matrix-assisted laser desorption ionization time-of-flight mass spectrometry (ABI, Perkin Elmer, Foster City, California, USA). The mass spectrometry was carried out in a linear and delayed-extraction mode. Internal and external calibrations were carried out using trypsin autolysis peaks and calibration mixtures (ABI), respectively.

Protein identification was achieved using MASCOT software (Mascot, Boston, Massachusetts, USA) with the most current National Center for Biotechnology Information nonredundant protein database.

Western blot analysis

To confirm the 2D electrophoresis results, mitochondrial proteins were separated by 12% SDS–PAGE and then blotted onto nitrocellulose membranes using a semidry transfer system. After blocking with 4% nonfat milk, the membranes were probed sequentially with primary and horseradish peroxidase-labeled secondary antibodies, and immunoreactive bands were detected with 3,3′-diaminobenzidine staining.

Results

Mitochondrial alterations

Mitochondria play an important role in the initiation of apoptosis including loss of MMP and release of apoptosis-related proteins (such as cytochrome *c*). We measured the alterations of MMP in HCPT-treated cells using the MitoCapture dye. Our data showed that 37% of the cells exhibited low MMP after their incubation with HCPT for 6 h (Fig. 1a).

To explore further the role of mitochondria during apoptosis, we observed the release of cytochrome *c* by a confocal microscope. Results suggested that cytochrome *c* was shown to localize in the mitochondria; however, cytochrome *c* was translocated into the cytosol after treatment with HCPT for 6 h (Fig. 1b).

The purity of mitochondria

To obtain mitochondria with high purity for its further application in proteome research, Janus green B staining was carried out to identify the mitochondrial fraction and Western blot analysis was applied to measure its purity. The results showed that there were some blue granules (Fig. 2a), and a little actin, histone, as well as cathepsin-D immunoreactivity were detectable in the mitochondrial fraction. These results demonstrate a good enrichment of mitochondria following mitochondria purification (Fig. 2b).

Analysis of the images of two-dimensional electrophoresis

Mitochondrial proteins were separated by 2D gel electrophoresis to around 600 protein spots that were recognized by the PDQuest software (PDI, Huntington Station, New York, USA) (Fig. 3a–d). The density of each spot was determined by the software and normalized against the total gel density, which represents the total protein quantity in the mitochondrial fraction. The experiment was carried out three times independently and the unpaired Student's *t*-test was performed to determine the statistically significant alterations. Fourteen and 25 protein spots were found to have an increased and a decreased abundance, respectively, in control cells compared with HCPT-treated cells. The *P* values for these spots in three independent experiments were less than 0.05.

Protein identification and differentially expressed proteins

Twenty-five spots were excised from a 2D gel, whereas about 14 spots with extremely faint densities were

Fig. 2

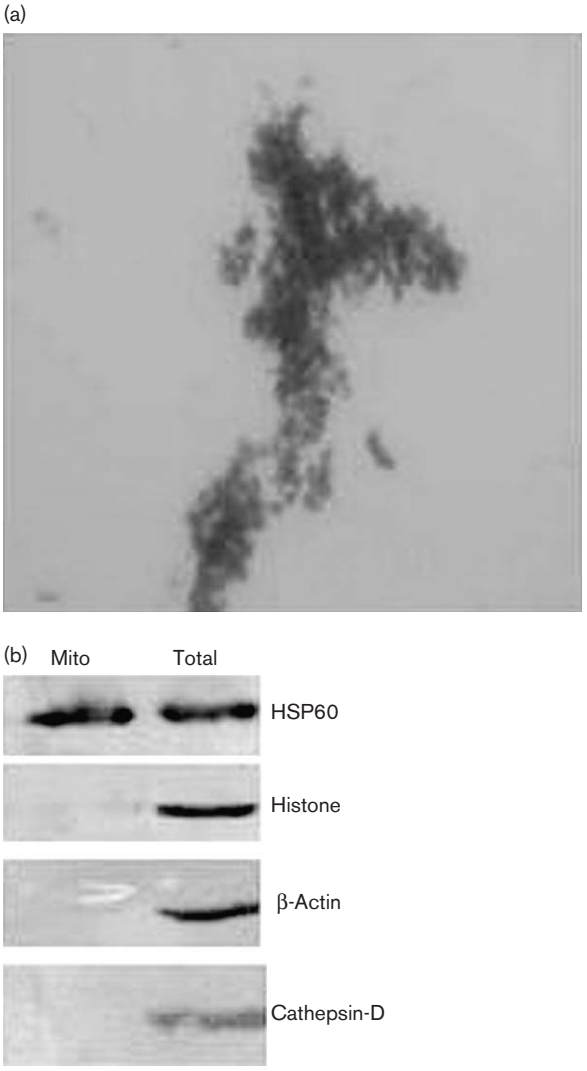

Detection of isolated mitochondrial purity. (a) Separated mitochondria were identified by Janus green B staining. (b) Purity of the isolated mitochondrial fractions was assessed by Western blot analysis with antibodies directed against proteins from various cellular locations. β-Actin, histone, and cathepsin-D immunoreactivity were detectable in small quantities in the mitochondrial fractions. Data represent results from three separate experiments. Mito, mitochondria fractions; Total, total cell extract.

omitted. In-gel tryptic digestion was performed and the extracted tryptic peptides were analyzed by the matrix-assisted laser desorption ionization time-of-flight mass spectrometry to generate peptide mass fingerprinting. Database searching with peptide mass fingerprinting was performed using the MASCOT algorithm to search the National Center for Biotechnology Information database. Top hits were precisely matched with the p*I*s and the molecular weights of predicted proteins. Thus, only closely matched values were taken into consideration for the identification of the proteins.

Fig. 3

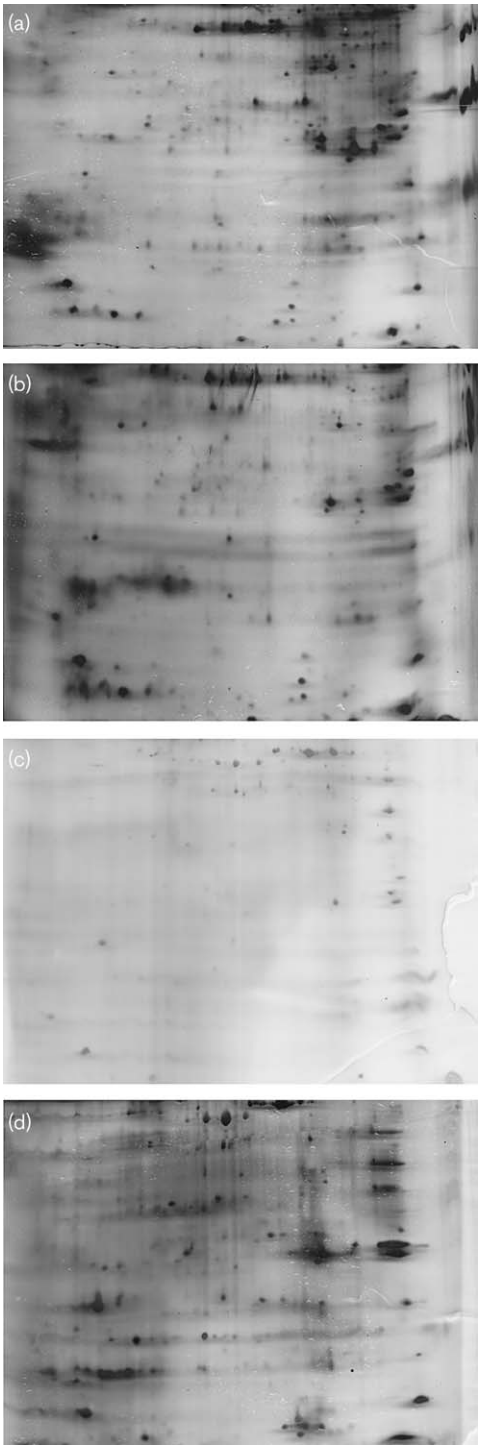

The two-dimensional (2D) protein maps of mitochondria. Mitochondrial proteins were separated by 2D gel electrophoresis to around 600 protein spots that were recognized by the PDQuest software. Fourteen and 25 protein spots were found to have an increased and a decreased abundance, respectively, in control cells compared with those in the HCPT-treated cells. The *P* values for these spots in three independent experiments were less than 0.05. (a, b) Fractions 1 of control mitochondria and apoptosis mitochondria, respectively; (c, d) fractions 2 of control mitochondria and apoptosis mitochondria, respectively.

Table 1 Functional classification of proteins isolated from two-dimensional electrophoresis gels of mitochondrial fractions and identification of 20 significantly changed proteins

Category	Protein	gi	M_r[a]	pI[a]
Cytoskeleton	Actin α	4501882	41 758	5.23
Cytoskeleton	Myosin, light polypeptide	62132964	22 521	5.03
Proliferation	Prohibitin	66267315	29 871	5.57
Apoptosis	AIF	83405866	66 539	9.03
Apoptosis	Cytochrome *c*	15219886	11 724	9.59
Apoptosis	Bax	23273683	24 375	7.74
Apoptosis	Drp1	6996005	82 396	6.37
Oxidative phosphorylation	Glycerol-3-phosphate dehydrogenase	20379680	38 066	5.81
Oxidative phosphorylation	ADP/ATP translocase 2	92090586	33 102	9.76
Oxidative phosphorylation	ATP synthase D chain	215952421	18 360	5.22
Oxidation	Cytochrome P450	38173818	59 782	9.18
Oxidation	Glutathione peroxidase	32967607	22 609	8.49
Oxidation	Glutathione S-transferase A2	12804085	25 531	8.54
Oxidation	Long-chain acyl-CoA synthetase	23273827	70 865	8.75
Oxidation	Diacylglycerol kinase	39645110	103 277	7.99
Oxidation	Coproporphyrinogen oxidase	23272125	40 836	8.5
Heat shock	HSP70	83406034	95 127	5.11
Heat shock	HSP10	23270723	10 794	8.91
Mitochondrial ribosome	S30	14043496	50 932	8.21
Mitochondrial ribosome	L43	31419637	18 528	9.75

The pI and mass values were obtained from the MASCOT database (gi, gene bank ID).
[a]Calculated value.

The 20 unique proteins that were identified from the 25 2D gel spots are listed in Table 1. Out of the 20 proteins, 12 proteins were upregulated, whereas eight proteins were downregulated in the presence of HCPT in the SMMC-7721 cells. The functions of the proteins in Table 1 are related to many essential cellular functions; they are mainly involved in the cytoskeleton structure; other functions include proliferation, apoptosis, oxidative phosphorylation, oxidation or antioxidant proteins, heat-shock proteins and mitochondrial ribosomes.

The two cytoskeleton proteins, including actin-α and myosin, displayed an increased abundance in HCPT-treated cells. Prohibitin, a proliferation-related protein, was identified and was found to have showed an increased abundance in HCPT-treated cells. It was expected that the amounts of apoptosis-inducing factor (AIF) and cytochrome *c*, apoptosis-related proteins, would be reduced in the mitochondria from apoptotic cells; however, it was a big surprise to note that the levels of the other two apoptosis-related proteins, Bax and Drp1, are also reduced. Out of the three oxidative phosphorylation proteins, ADP/ATP translocase 2 chain and ATP synthase D were increased in expression, whereas glycerol-3-phosphate dehydrogenase was decreased in expression. Six oxidation-related proteins were identified, i.e. glutathione S-transferase A2, cytochrome P450, diacylglycerol kinase, glutathione peroxidase, coproporphyrinogen oxidase and long-chain acyl-CoA synthetase, out of which diacylglycerol kinase was downregulated, whereas the other five proteins were upregulated in HCPT-treated cells. Two heat-shock proteins, including HSP10 and HSP70, were identified and they showed increased levels in HCPT-treated cells. L43 and S30, the mitochondrial ribosomal proteins, were downregulated in HCPT-treated cells.

Confirmation of differential expression levels of protein by Western blot

To confirm the 2D results, two interesting proteins, AIF and actin, were selected and subjected to Western blot analysis. The data (Fig. 4) showed that actin (Fig. 4a) had an increased abundance and AIF had a decreased abundance (Fig. 4b), whereas HSP60 (Fig. 4c) showed no significant changes in the mitochondria from the HCPT-treated cells. It is known that both Bax and Drp1 are translocated and accumulated in the mitochondria during apoptosis. Therefore, Western blot analysis was applied to validate the unusual result. It is noted that both Drp1 and Bax had an increased abundance when the cells were incubated with HCPT for 3 h, whereas both had a decreased abundance when incubated for 6 and 8 h, respectively (Fig. 5).

Discussion

Subcellular fractionation is a flexible and adjustable approach resulting in reduced sample complexity and is most efficiently combined with high-resolution 2D gel/mass spectrometry analysis as well as with gel-independent techniques [9–11]. Mitochondria are ubiquitous organelles responsible for the energy metabolism of eukaryotic cells. More recent studies suggest an additional role of the mitochondrion in ionic homeostasis, apoptosis and aging [12–14]. These findings have promoted increasing efforts to define the mitochondrial proteome and to discover new molecular targets for drug development and therapeutic intervention [15].

Fig. 4

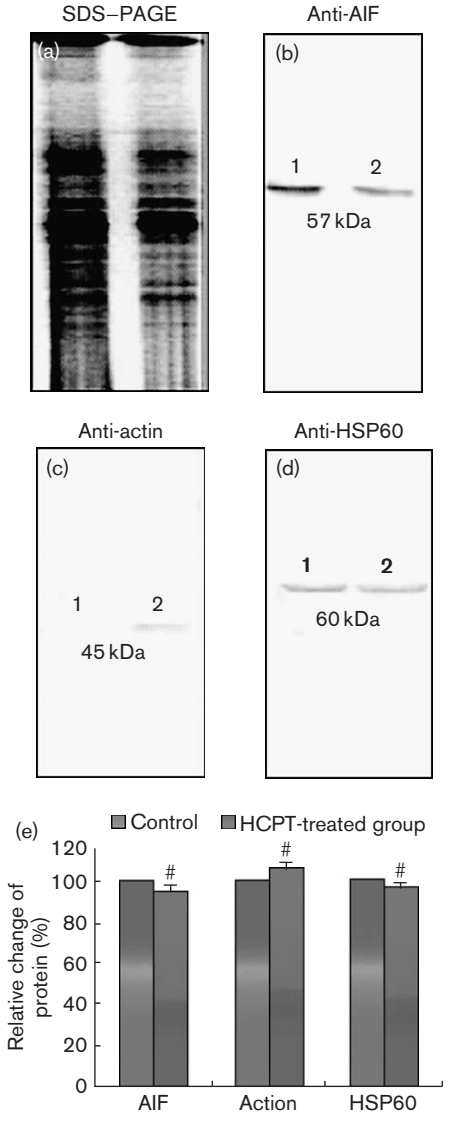

Expression levels of AIF and actin in the mitochondria. (a) SDS–PAGE for standardization of proteins of mitochondria; (b–d) detection of expression levels of AIF, actin, and HSP60, respectively; 1: control; 2: HCPT-treated group; E: histogram of two different protein patterns in control and mitochondria from apoptotic cells. $^{\#}P<0.05$ versus control. AIF, apoptosis-inducing factor; HCPT, hydroxycamptothecin.

Fig. 5

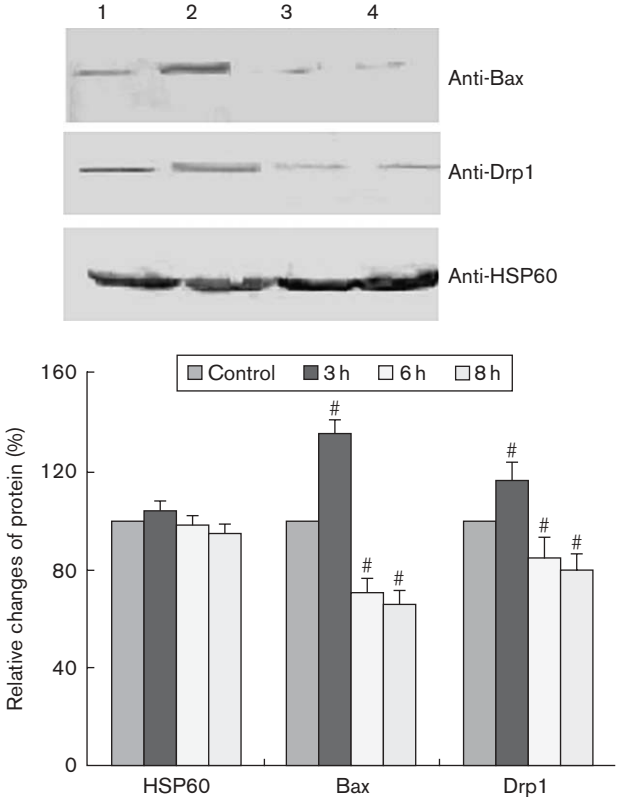

Western blot analysis of Bax and Drp1. Bax and Drp1 concentrations in mitochondria were analyzed by Western blot. Both Drp1 and Bax were found to be increased after treatment for 3 h, whereas both were found to be decreased after treatment for 6 and 8 h. 1: Control; 2: HCPT treatment for 3 h; 3: HCPT treatment for 6 h; 4: HCPT treatment for 8 h. $^{\#}P<0.05$ vs. control. HCPT, hydroxycamptothecin.

The purity of subcellular fractions is crucial to subcellular proteome research [16]. Many assays can be used to assess the results of subcellular fractionation experiments. First, quantitative Western blot can be used to analyze the distribution of specific organelle marker proteins. Second, for morphological analysis of all fractions, standard microscope procedures can be applied. In this study, both Western blot and morphological analysis were used to evaluate the purity of the isolated mitochondrial fraction [17].

To enrich the low-abundant proteins and to reduce the complexity of the samples, the sequential extraction approach was used for preparing the mitochondrial proteins. Thirty-nine 2D gel spots displayed an altered abundance between the mitochondrial fractions isolated from the HCPT-treated and those from untreated cells. Twenty-five of the 39 2D gel spots represented 20 distinct proteins, which are listed in the supplementary table. The functions of these proteins that have been annotated in the EXPASY and Proteome BioKnowledge databases include cytoskeleton structuring, proliferation, apoptosis, oxidative phosphorylation, redox reactions, and those of antioxidant proteins heat-shock proteins and mitochondrial ribosomes.

Some mitochondrial shape transitions are linked to disease or apoptosis. Changes in the cytoskeleton structure have recently been considered to be another typical feature of apoptosis [18]. In our study, actin and myosin were involved in HCPT-mediated apoptosis,

which suggested that HCPT could initiate mitochondrial shape transitions.

Prohibitin, an evolutionarily conserved protein located in the inner membrane of the mitochondria, is a potential tumor suppressor that can repress E2F1-mediated transcription and arrest cell proliferation [19]. Our findings showed that prohibitin was upregulated in HCPT-treated cells. Among oxidative phosphorylation proteins, glycerol-3-phosphate dehydrogenase showed a decrease in expression, whereas ADP/ATP translocase 2 chain and ATP synthase D both showed increases in expression. Out of the three oxidative phosphorylation proteins, glycerol-3-phosphate dehydrogenase had a decreased abundance, whereas ADP/ATP translocase 2 chain and ATP synthase D had an increased abundance in HCPT-treated cells. It is well known that the ADP/ATP translocator can regulate the mitochondrial permeability-transition pore (PTP). The modification of PTP showed a decreased level in HCPT-treated cells, which might lead to a regulation of cytochrome *c*, AIF release and activation of apoptosis. The decrease of cytochrome *c* and AIF during HCPT-mediated apoptosis might be associated with their release from mitochondria when PTP was reduced. It is a big surprise that the levels of two other apoptosis-related proteins, Bax and Drp1, were also decreased. It is known that both Bax and Drp1 are translocated and accumulated in the mitochondria during apoptosis. These unusual results were further validated by Western blot analysis. Interestingly, both Drp1 and Bax were increased when cells were treated with HCPT for 3 h, whereas both were decreased when cells were treated for 6 and 8 h. Little is known about the mechanisms.

It is well known that many enzyme systems participate in the regulation of apoptosis. The results showed that there was a marked increase in some oxidation-related proteins after treatment with HCPT, which might be associated with the accumulation of damage from mitochondrial oxygen radicals [20]; the expression of diacylglycerol kinase was, however, decreased and the underlying mechanism is still not clear. HSP70 participates in processes including protein synthesis, protein translocation across mitochondrial membranes and protein folding [21]. Moreover, increasing evidence displays its important role against apoptosis by inducing drug resistance. HSP10 can modulate the bcl-2 family and the mitochondrial apoptosis signals, which can explain our findings of relatively high levels of HSP70 and HSP10 during apoptosis induced by HCPT. Mitochondrial ribosomal proteins were involved in regulating cell apoptosis and their expressions were generally high in cancer cells, which can explain our findings that mitochondrial ribosomal protein L43 and S30 had a decreased abundance in HCPT-treated cells.

Conclusion

Subcellular proteome analysis provides an effective approach for elucidating the role of HCPT. The findings in this study provide a comprehensive knowledge of the mitochondrial proteome in HCPT-treated cells, which has a broad impact on the research of the mechanism by which HCPT induces cell apoptosis. It has laid the ground for further studies to elucidate the role of particular mitochondrial proteins, such as Drp1, in HCPT-mediated apoptosis.

Supplementary data

Supplementary data are available at *Anti-Cancer Drugs* Online (http://www.anticancerdrugs.com).

Acknowledgements

The authors thank Dan Zhu, Qiang Yang, Shu-Hui Chen and Ming-Fang Liu for technical support. The authors also thank Yan Wang and Lian-fen Huang for their critical reading of the manuscript.

References

1 Zhang ZW, Patchett SE, Farthing MJ. Topoisomerase I inhibitor (camptothecin)-induced apoptosis in human gastric cancer cells and the role of wild-type p53 in the enhancement of its cytotoxicity. *Anti cancer Drugs* 2000; **11**:57–64.

2 Widlak P, Li LY, Wang X, Garrard WT. Action of recombinant human apoptotic endonuclease G on naked DNA and chromatin substrates: cooperation with exonuclease and DNase I. *J Biol Chem* 2001; **276**:48404–48409.

3 Ajani JA. Current status of therapy for advanced gastric carcinoma. *Oncology* 1998; **12**:99–102.

4 Jin Z, El-Deiry WS. Overview of cell death signaling pathways. *Cancer Biol Ther* 2005; **4**:139–163.

5 Joza N, Susin SA, Daugas E, Stanford WL, Cho SK, Li CY, *et al.* Essential role of the mitochondrial apoptosis-inducing factor in programmed cell death. *Nature* 2001; **410**:549–554.

6 Fu YR, Yi ZJ, Yan YR, Qiu ZY. Hydroxycamptothecin-induced apoptosis in hepatoma SMMC-7721cells and the role of mitochondrial pathway. *Mitochondrion* 2006; **6**:211–217.

7 Kiri AN, Tran HC, Drahos KL, Lan W, McRorie DK, Horn MJ. Proteomic changes in bovine heart mitochondria with age: using a novel technique for organelle separation and enrichment. *J Biomol Tech* 2005; **16**:371–379.

8 Rabilloud T, Strub JM, Carte N, Luche S, van Dorsselaer A, Lunardi J, *et al.* Comparative proteomics as a new tool for exploring human mitochondrial tRNA disorders. *Biochemistry* 2002; **41**:144–150.

9 Huber LA, Pfaller K, Vietor I. Organelle proteomics: implications for subcellular fractionation in proteomics. *Circ Res* 2003; **92**:962–968.

10 Pasquali C, Fialka I, Huber LA. Subcellular fractionation, electromigration analysis and mapping of organelles. *J Chromatogr B Biomed Sci Appl* 1999; **722**:89–102.

11 Fialka I, Pasquali C, Lottspeich F, Ahorn H, Huber LA. Subcellular fractionation of polarized epithelial cells and identification of organelle specific proteins by two-dimensional gel electrophoresis. *Electrophoresis* 1997; **18**:2582–2590.

12 Fossati G, Moulding DA, Spiller DG, Moots RJ, White MR, Edwards SW. The mitochondrial network of human neutrophils: role in chemotaxis, phagocytosis, respiratory burst activation, and commitment to apoptosis. *J Immunol* 2003; **170**:1964–1972.

13 Piana G La, Marzulli D, Consalvo MI, Lofrumento NE. Cytochrome *c*-induced cytosolic nicotinamide adenine dinucleotide oxidation, mitochondrial permeability transition, and apoptosis. *Arch Biochem Biophys* 2003; **410**:201–211.

14 Jambrina E, Alonso R, Alcalde M, del Carmen Rodriguez M, Serrano A, Martinez-A C, *et al.* Calcium influx through receptor-operated channel induces mitochondria-triggered paraptotic cell death. *J Biol Chem* 2003; **278**:14134–14145.

15 Fountoulakis M, Berndt P, Langen H, Suter L. The rat liver mitochondrial proteins. *Electrophoresis* 2002; **23**:311–328.
16 Dunkley TP, Dupree P, Watson RB, Lilley KS. The use of isotope-coded affinity tags (ICAT) to study organelle proteomes in Arabidopsis thaliana. *Biochem Soc Trans* 2004; **32**:520–523.
17 Huber LA, Pfaller K, Vietor I. Organelle proteomics: implications for subcellular fractionation in proteomics. *Circ Res* 2003; **92**:962–968.
18 Gourly CW, Ayscough KR. Identification of an upstream regulatory pathway controlling actin-mediated apoptosis in yeast. *J Cell Sci* 2005; **118**: 2119–2132.
19 Joshi B, Ko D, Ordonez-Ercan D, Chellappan SP. A putative coiled-coil domain of prohibitin is sufficient to repress E2F1-mediated transcription and induce apoptosis. *Biochem Biophys Res Commun* 2003; **312**: 459–466.
20 Back JW, Sanz MA, de Jong L, de Koning LJ, Nijtmans LG, de Koster CG, *et al*. A structure for the yeast prohibitin complex: structure prediction and evidence from chemical crosslinking and mass spectrometry. *Protein Sci* 2002; **11**:2471–2478.
21 Liu Q, Krzewska J, Liberek K, Craig EA. Mitochondrial Hsp70 Ssc1: role in protein folding. *J Biol Chem* 2001; **276**:6112–6128.